Secondary Minimum Coagulation in Charged Colloidal Suspensions from Statistical Mechanics Methods

María Cortada,[†] Juan A. Anta,*[,†] and J. A. Molina-Bolívar[‡]

Departamento de Sistemas Físicos, Químicos y Naturales, Área de Química-Física, Universidad "Pablo de Olavide", Ctra. de Utrera, Km. 1, 41013 Sevilla, Spain, and Departamento de Física Aplicada II, Escuela Universitaria Politécnica, Universidad de Málaga, Campus de El Ejido, s/n, 29013, Málaga, Spain

Received: September 20, 2006; In Final Form: November 24, 2006

A statistical mechanics approach is applied to predict the critical parameters of coagulation in the secondary minimum for charged colloidal suspensions. This method is based on the solution of the reference hypernetted chain (RHNC) integral equation, and it is intended to estimate only the locus of the critical point instead of the full computation of the "gas−liquid" coexistence. We have used an extrapolation procedure due to the lack of solution of the integral equation in the vicinity of the critical point. Knowing that the *osmotic* isothermal compressibility of the colloidal system should ideally diverge in the critical point, we work out the critical salt concentration for which the inverse of the compressibility should be zero. This extrapolation procedure is more rapid than that previously proposed by Morales and co-workers [Morales, V.; Anta, J. A.; Lago, S. *Langmuir* **2003**, *19*, 475], and it is shown to give equivalent results. We also present experimental results about secondary minimum coagulation for polystyrene latexes and use our method to reproduce the experimental trends. The comparison between theory and experiment is quite good for all colloidal diameters studied.

I. Introduction

One of the key issues in the application of colloid science in chemistry, biology, and technology is the stability of a colloidal suspension.[1,46] A major problem consists of predicting the stability properties of colloidal systems starting from the nature of the colloids, the experimental conditions, and the specific form of their interaction forces.

In this regard, the Derjaguin−Landau−Verwey−Overbeek (DLVO) interaction potential[2,3] represents a very powerful instrument to predict the stability of charged colloidal suspensions. The DLVO pair interaction has two components: (1) van der Waals attraction and (2) electrostatic repulsion. The interplay between them leads to a potential energy function that exhibits a deep primary minimum at short distances, a positive potential barrier at intermediate distances, and a shallow secondary minimum at large distances. In this work we focus on the case of coagulation in the secondary minimum. In contrast to the well-studied case of coagulation in the primary minimum, the DLVO theory on its own is not capable of predicting when coagulation in the secondary minimum will take place for given salt concentration and system. An extra theory is needed to solve the statistical mechanics problem posed by the DLVO interaction potential. This difficulty was already mentioned by Verwey and Overbeek in their classic book[3] and studied theoretically by Grimson,[4] Victor and Hansen,[5] Kaldasch et al.,[6] Lai and co-workers,[7,8] Wu and Lai,[9] and some of us.[10]

Theoretical prediction of secondary minimum coagulation is habitually performed starting from an effective one-body potential (like the DLVO) and assuming that the colloidal aggregation can be regarded as a "gas−liquid" thermodynamic transition. Thus, the salt concentration plays the role of an inverse temperature: if this goes *above* a certain *critical* value, the system ceases to be stable and separates into two phases. Hence it is possible to calculate a "gas−liquid" coexistence curve and predict the existence of a critical point.

Experimentally, coagulation in the secondary minimum is normally observed in the form of *repeptization*. Repeptization is the situation that a colloid, after having been aggregated, can be redispersed by washing away the aggregating salt.[11] For this reason coagulation in the secondary minimum is normally referred to as *reversible coagulation*, in contrast to the *irreversible coagulation* that takes place in the primary minimum. When aggregation occurs in a deep primary minimum, the particle surface can come into intimate contact. In the case of coagulation in the secondary minimum, a liquid film is retained between the particles, and the depth of the energy well is much smaller. Hence, the aggregation in the secondary minimum should be reversible upon salt dilution since the secondary well can be reduced by decreasing the ionic strength.[12−14]

Secondary minimum coagulation becomes the preferential aggregation mechanism for ordinary DLVO particles with large colloidal diameters.[10,15] It has been also reported as the main coagulation mechanism in systems with large potential barriers[16] or where the primary minimum does not exist at all.[17] Secondary minimum coagulation has been also mentioned recently as a possible cause of colloidal deposition in porous media.[18] In all these situations it is very important to have a numerical procedure that provides quick and accurate predictions of the stability properties for a given interaction potential. In addition, the availability of a good thermodynamic theory to describe this phenomenon opens the way to using its results as input data to compute kinetic rate constants.[9] As we will see below, colloid−colloid radial distribution functions can provide interesting information in this context.

In a previous work we employed an integral equation approach to obtain the coagulation properties of the DLVO potential.[10] Integral equation theories[19,20] are particularly useful

[†] Universidad "Pablo de Olavide".
[‡] Universidad de Málaga.

10.1021/jp0661589 CCC: $37.00
Published on Web 01/11/2007

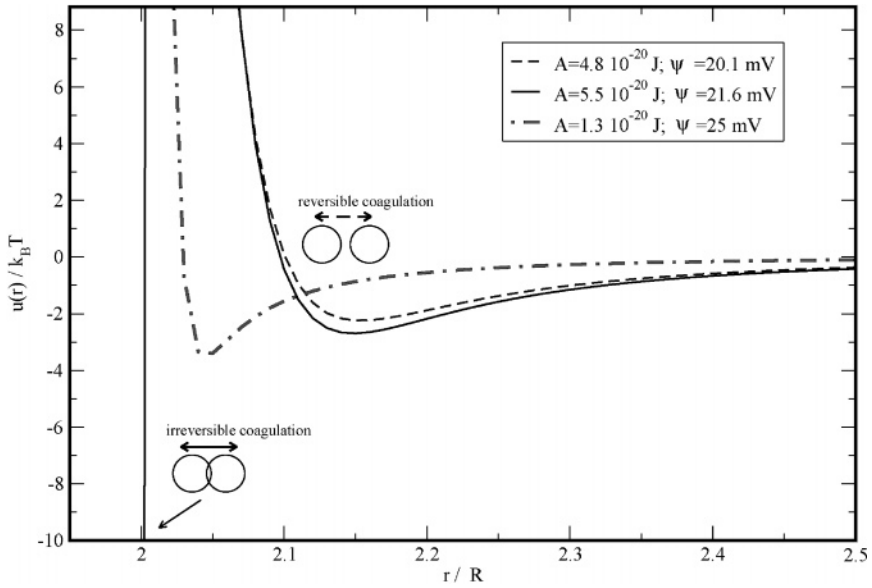

Figure 1. DLVO interaction potentials for colloidal dispersions studied in ref 10. Only the energy barrier and secondary minimum region are represented. The potential is plotted in reduced units of energy (k_BT) and distance ($R = D/2$) for the critical salt concentrations that yield reversible coagulation with the RHNC integral equation (see Table 3).

in the field of the statistical mechanics of fluids due to their accuracy and low computational demands. We make use here of the reference hypernetted chain (RHNC) integral equation, a theoretical approach that has been shown to be especially accurate in reproducing the structure and thermodynamic properties of simple liquids,[21−23] liquid metals,[24] and molecular fluids.[25] The RHNC theory has also been applied successfully to obtain gas−liquid coexistence curves for a variety of cases,[22,26] including the (DLVO-like) hard-core Yukawa potential.[23] Integral equations can also be applied outside the effective component representation and used to predict the stability from a more fundamental point of view.[27,28] In this work we present an alternative method to predict secondary minimum coagulation. As shown by comparison with Monte Carlo simulation, the method proposed previously[10] provided quite accurate results for the "gas−liquid" coexistence curve of DLVO systems. Nevertheless this method becomes sometimes very cumbersome, especially when the nonsolution line of the integral equation interferes with the phase coexistence line. To avoid this drawback, we have devised a procedure intended to predict only the locus of the critical point. This is particularly appealing within the issue of colloidal stability since in this case one just wants to find out the critical salt concentration of reversible coagulation. Hence the computation of the full coexistence line is not required. Our method is based on the diverging properties of the osmotic[29] isothermal compressibility in the critical point. By extrapolation it is possible to estimate the critical parameters. This indirect method is shown to give results equivalent to those of the more elaborate procedure. We also present an extensive test of the method by comparing previous[30] and new experimental results of critical concentration of repeptization for various colloidal diameters.

II. Model Interaction Potential and RHNC Theory

(a) Effective One-Component System and Modified DLVO Potential. As mentioned in the Introduction, the present study is based on the assumption that the original colloidal mixture is reduced to an effective one-component system characterized by a single one-body potential $u(r)$, with r being the distance between the centers of mass of two colloidal particles. A more detailed description of the definition of the effective potential has been given elsewhere.[28,29,31−33] The purpose of this procedure is to transform the colloid−ion mixture into a colloidal "gas". Once the effective potential reduction is implemented, the thermodynamic properties that can be obtained from this potential will be *osmotic*; i.e., they correspond to the system of colloids on its own and defined with respect to a reservoir containing only salt ions and solvent molecules.[29]

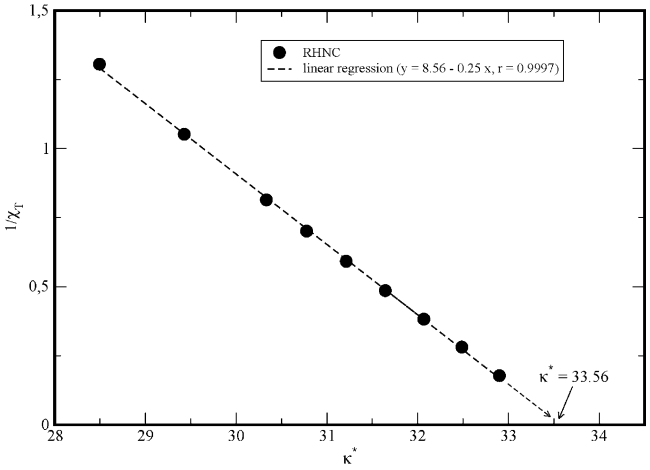

Figure 2. Inverse of the osmotic isothermal compressibility as a function of the Debye parameter in reduced units ($\kappa^* = \kappa R$, with R being the colloidal radius) for one of the systems defined in Table 3 ($A = 5.5 \times 10^{-20}$ J and $\psi_0 = 21.6$ mV). The value of the critical Debye parameter obtained by extrapolation is indicated with an arrow.

In this work we focus on the DLVO effective pair potential,[3] although the procedures described below can be also applied to other interactions as well as for other versions of the DLVO potential.[1,46] For an ensemble of colloidal particles of diameter D immersed in a polar solvent and in the presence of added salt, the DLVO interaction is

$$u_{DLVO}(r) = u_A(r) + u_R(r) \quad (1)$$

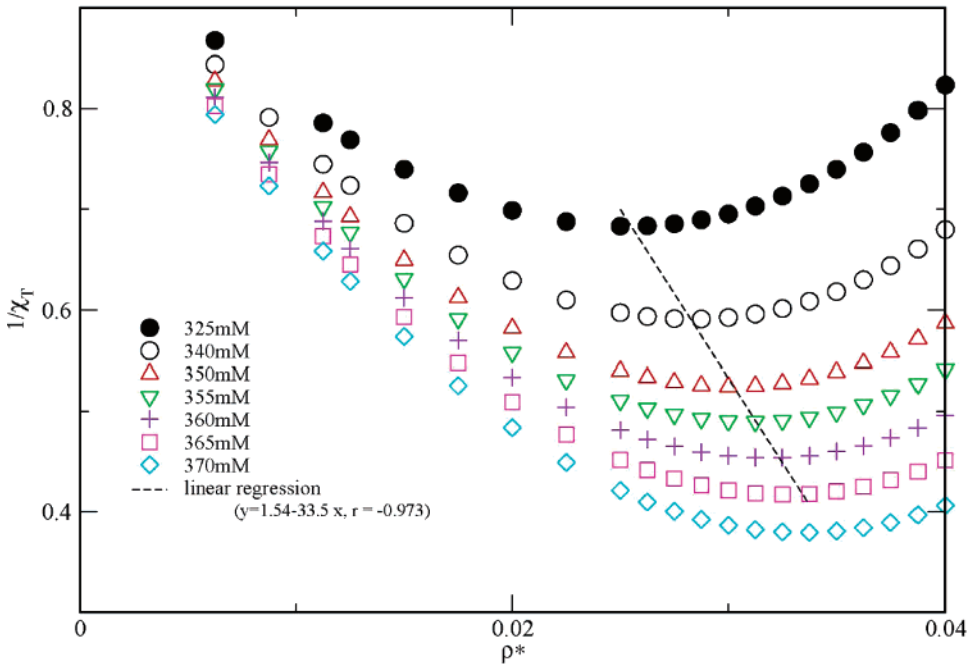

Figure 3. Inverse of the osmotic isothermal compressibility versus colloidal concentration in reduced units ($\rho^* = \rho R^3$, with R being the colloidal radius) for the same system as in Figure 2. The critical colloidal concentration obtained from extrapolation of the curve minima is $\rho_c^* = 0.046$ in this case.

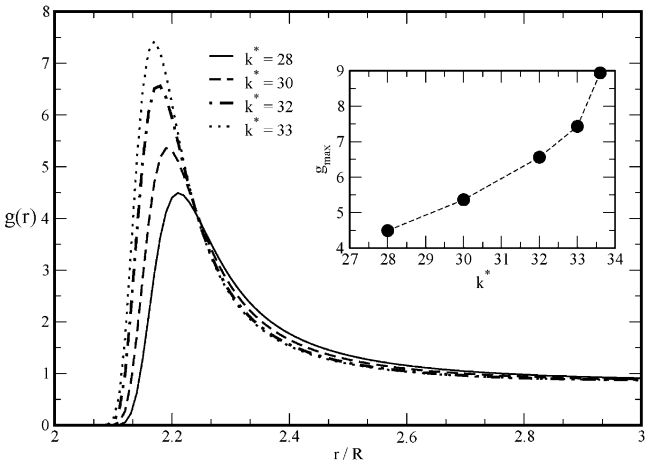

Figure 4. Radial distribution functions for the same case studied in Figure 2. In the inset, the maxima of $g(r)$ for each Debye parameter ($\kappa^* = \kappa R$) is presented.

where $u_A(r)$ corresponds to the van der Waals attraction

$$u_A(r) = -\frac{A}{12}\left[\frac{D^2}{r^2 - D^2} + \frac{D^2}{r^2} + 2\ln\left(1 - \frac{D^2}{r^2}\right)\right] \qquad (2)$$

with A being the Hamaker constant, and $u_R(r)$ represents the double-layer repulsion due to the salt ions. Following Kaldasch et al.[6] we have used the linear superposition approximation[1,46] to describe this electrostatic interaction. Solving the Poisson−Boltzmann equation for spherical particles at constant surface potential ψ_0, the following equation is obtained:

$$u_R(r) = \frac{16\pi\epsilon D^2}{e^2}\left[k_B T \tanh\left(\frac{e\psi_0}{4k_B T}\right)\right]^2 \frac{\exp(-\kappa(r - D))}{r} \qquad (3)$$

where e is the elementary charge, k_B is the Boltzmann constant, and T is the absolute temperature. For small values of ψ_0, eq 3 can be approximated by

$$u_R(r) = \pi\epsilon D^2 {\psi_0}^2 \frac{\exp(-\kappa(r - D))}{r} \qquad (4)$$

where ϵ is the dielectric constant of the solvent and κ is the inverse Debye length

$$\kappa = \sqrt{\frac{e^2}{\epsilon k_B T}\sum_i \rho {z_i}^2} \qquad (5)$$

with z_i and ρ_i being the valence and the density of all *charged* species i present in the sample.

The DLVO potential defined by eqs 1, 2, and 4 is plotted in Figure 1 for several colloidal systems. Although not shown in the figure, one of the main features of this potential is the attractive primary minimum a short distances. As this primary minimum is infinitely deep and the positive potential barrier is always finite, the colloidal system as described by the DLVO potential is *thermodynamically unstable* so that the equilibrium state of the suspension is the *coagulated* state. Only if the positive potential barrier is high enough with respect to the average thermal energy of the particles can coagulation in the primary minimum be slow enough to stabilize effectively the system. Thus, the system becomes *kinetically* stable although thermodynamically unstable. Nevertheless, if we apply a purely thermodynamic or equilibrium method such as the RHNC theory, we will be always predicting irreversible coagulation even if this is not the case in practical terms. To avoid this problem, Victor and Hansen[5] ignored completely the primary minimum by replacing the short-range behavior of the DLVO potential by a purely repulsive interaction. Following this strategy, we take a modified DLVO potential defined by

$$u(r) = \begin{cases} \infty & r < r_{max} \\ u_{DLVO}(r) & r > r_{max} \end{cases} \qquad (6)$$

where r_{max} corresponds to the position of the positive energy barrier. Obviously this scheme for replacing a kinetically stable

TABLE 1: Main Characteristics of the Latexes Studied in This Work

			ccc (mM)	
latex	D^a (nm)	PDI	NaCl	$CaCl_2$
MP2	361 ± 14	1.005		75 ± 8
Lx1	414 ± 14	1.003	433 ± 40	78 ± 8
Lx2	530 ± 18	1.004	275 ± 30	
AS11	661 ± 18	1.002	148 ± 10^b	

[a] From TEM. [b] Data from ref 30.

system by a thermodynamically stable one is only valid if the potential barrier is very high in comparison with the average thermal energy of the particles, that is,[5] $u_{DLVO}(r_{max}) > 10k_BT$ or[7] $u_{DLVO}(r_{max}) > 15k_BT$. In this work we have taken the first of these values as a convenient choice. Nevertheless, we should bear in mind that the results presented here should be taken with some caution when the energy barrier approaches this limit. For smaller values of the height of the energy barrier, we should assume that there is a somehow indefinite region where irreversible and reversible coagulation will coexist. A more comprehensive analysis of this issue has been carried out by Wu and Lai.[9]

(b) RHNC Theory of Simple Liquids. The RHNC theory is a statistical mechanics[19] technique which relies on the assumption that the system is in thermodynamic equilibrium. For a *one-component system* the theory applies to a collection of N particles that interact via a pairwise additive potential $u(r)$. Under these prescriptions the microscopic structure and thermodynamics of the system is completely determined by the radial distribution function $g(r)$. In the canonical ensemble, i.e., for number of particles N, volume V and T fixed, this is defined by[19]

$$g(r) = \frac{V^2 \int d\mathbf{r}^{N-2} \exp[-\beta \sum_{i<j} u(r_{ij})]}{\int d\mathbf{r}^{N} \exp[-\beta \sum_{i<j} u(r_{ij})]} \quad (7)$$

with $\beta = 1/k_BT$. The RHNC theory provides an approximate but highly accurate way to obtain $g(r)$. Starting from a functional Taylor expansion of the excess free energy in terms of density derivatives,[19,34] it is possible to express $g(r)$ in the form

$$g(r) = \exp[-\beta u(r) + h(r) - c(r) - B(r)] \quad (8)$$

where $h(r) = g(r) - 1$ and $c(r)$, the direct correlation function, can be defined via the Ornstein−Zernike equation[19,20]

$$h(r) = c(r) + \rho \int c(|\mathbf{r} - \mathbf{r}'|)\, h(r')\, d\mathbf{r}' \quad (9)$$

where ρ ($=N/V$) is the number density of particles and $B(r)$ is the bridge function, which is related to the higher-than-two density functional derivatives of the excess free energy. If we assume $B(r) = 0$, eqs 8 and 9 constitute a closed relation that determines $g(r)$ for given temperature and density. This is the HNC approximation. Within the RHNC scheme, the bridge function is not neglected but is assumed to be equal to the bridge function of a suitable reference system.[35] Customarily this reference potential is taken to be the hard-sphere potential, which is defined by a single parameter, the hard-sphere diameter σ. Thus, in the RHNC approximation[36]

$$B(r) \approx B^0(r;\sigma) \quad (10)$$

where $B^0(r;\sigma)$ is the bridge function of a fluid of hard spheres of diameter σ. Now eqs 8−10 define the $g(r)$ for given temperature and density, provided we have the means to specify the optimum hard-sphere diameter σ. In this work we fix this parameter using the optimization criterium of Lado, Foiles, and Ashcroft,[37] the hard-sphere radial distribution function of Verlet and Weis,[38] and the hard-sphere bridge function $B^0(r;\sigma)$ of Labík and Malyjevský.[39]

The RHNC integral equation is solved numerically using fast Fourier transform methods. In the numerical solution of the integral equation the correlation functions are tabulated on a grid of 4096 points with a grid size of $0.005D$ in real space. An iterative procedure is then employed to obtain the final solution for $g(r)$. The method of Ng[40] combined with Broyles' strategy[41] to mix conveniently successive estimates of the correlation functions is employed to enhance convergence. A superposed iterative procedure is implemented to obtain the optimum hard-sphere diameter σ. To do this, we start from an initial value of $\sigma = D$, where D is the colloidal diameter itself. The final converged solution for a given thermodynamic point defined by T, ρ, and κ takes a few seconds in a standard computer. To obtain a converged solution for points of high densities or high Debye constant, it might be necessary to start from a previous solution obtained at a lower density or lower Debye constant.

(c) Estimation of the Critical Point from the Solution of the RHNC Integral Equation. In this work we make use of the fact that the osmotic isothermal compressibility χ_T diverges in the proximity of the critical point. Since χ_T depends explicitly only on the colloid−colloid correlations[29] and these are determined by the form of the effective potential,[27] coagulation in the secondary minimum should be associated with a infinity value of χ_T. This is defined by[29]

$$\chi_T = -\frac{1}{V}\frac{\delta V}{\delta \Pi} \quad (11)$$

where Π is the osmotic pressure of the colloidal system. Within the RHNC approach χ_T is obtained from the compressibility equation[19]

$$\rho k_B T \chi_T = 1 + \rho \int (g(r) - 1)\, d\mathbf{r} \quad (12)$$

Thus, if the colloid−colloid correlations represented by $g(r) - 1$ become infinite as a consequence of the approach to the critical point, the isothermal compressibility should also reach an infinite value.

The RHNC integral equation cannot be solved in the proximity of the critical region. Nevertheless, we can estimate the locus of the critical point by extrapolation. In Figure 2 it is shown how the inverse of the isothermal compressibility goes toward zero as we approach the critical Debye constant. The RHNC results fit very nicely to a straight line. This means that the corresponding critical exponent adopts a classical[42] value of $\delta = 1$. This is not surprising since RHNC results usually exhibit linear behavior when one approaches the critical point by varying the temperature.[20,43] A more careful analysis of the

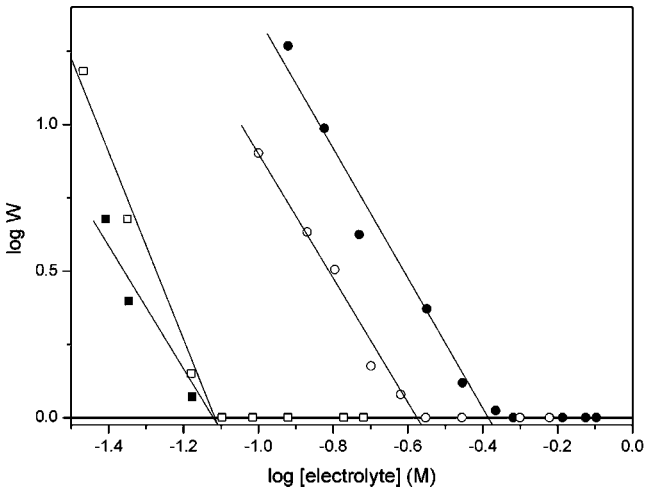

Figure 5. Dependence of the stability factor (W) on the electrolyte concentration for (■) MP2 with $CaCl_2$, (□) Lx1 with $CaCl_2$, (●) Lx1 with NaCl, and (○) Lx2 with NaCl.

TABLE 2: Reversibility of Salt-Induced Aggregation for the Latexes Measured by PCS[a]

electrolyte concn (mM)	MP2	Lx1	Lx2	AS11
5 (Ca^{2+})	–	–		
10 (Ca^{2+})	yes	yes		
20 (Ca^{2+})	yes	yes		
50 (Ca^{2+})	no	no		
25 (Na^{+})				–
33 (Na^{+})		–	–	yes
45 (Na^{+})		–	yes	yes
70 (Na^{+})		yes	yes	yes
400 (Na^{+})		yes	no	no
500 (Na^{+})		no	no	no

[a] "Yes", repeptization occurs; "no", repeptization does not occur; "–", no aggregation observed.

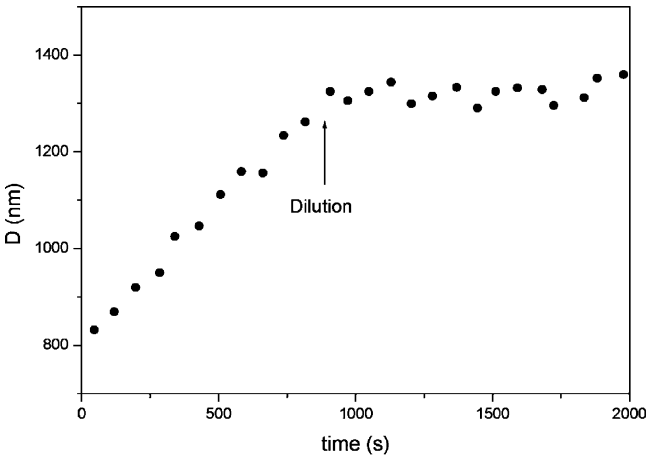

Figure 6. Aggregate average diameter (D) versus time for the system Lx1 in 50 mM $CaCl_2$.

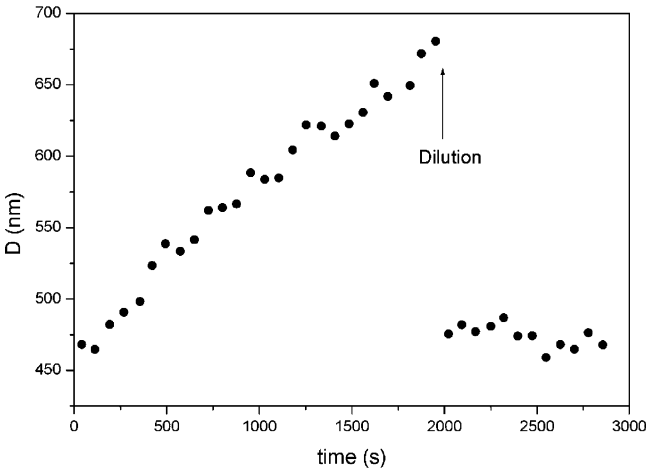

Figure 7. Aggregate average diameter (D) versus time for the system Lx1 in 400 mM NaCl.

approach to the critical temperature is presented in the Appendix for a model fluid.

The calculation of Figure 2 is performed at the critical colloidal density ρ_c. This is obtained in turn by looking at the minima of $1/\chi_T$ when it is plotted as a function of ρ. The best value of the critical colloidal density is also extracted by extrapolation to the colloidal density for which the inverse of the isothermal compressibility is ideally zero (see Figure 3).

In summary we use the following procedure:

Step 1: We search for the critical colloidal density ρ_c by solving the RHNC integral equation along an "isotherm", that is, for fixed Debye constant κ. This calculation is repeated for increasing Debye parameters (increasing salt concentrations), and the minima of the corresponding isotherms are recorded. The values of these minima are used to estimate ρ_c by extrapolation (see Figure 3).

Step 2: Once the value of ρ_c is known, we solve the RHNC equation along a critical "isochore" (constant value of ρ_c). The calculation is started at small values of the Debye constant κ, and then its value is gradually increased by small steps until the integral equation ceases to have a solution.

Step 3: The value of the critical Debye constant κ_c is then estimated by extrapolation from the representation of $1/\chi_T$ versus κ for the critical isochore obtained in step 2 (see Figure 2). The value of κ_c so obtained determines the concentration of salt above which the system coagulates (reversibly) in the secondary minimum.

The accuracy of this numerical procedure is limited by the behavior of the RHNC integral equation in the vicinity of the critical region. In this respect it must be pointed out that the HNC and RHNC integral equations exhibit nonsolution boundary lines which do not behave as true spinodals.[44] Hence it could be objected that estimating the locus of the critical point by extrapolation of the inverse of χ_T to zero could not be accurate because the integral equations do not present diverging values of this magnitude when the nonsolution boundary is approached. However, this anomalous behavior only affects the region very close to the nonsolution boundary. As a matter of fact, and due to the approximate nature of this theory, the numerical solution of the integral equation can even yield nonphysical values of the thermodynamic quantities as we approach the nonsolution region. These values should be discarded if we want to obtain a good estimation of the critical point.

The nature of the nonsolution line of Ornstein–Zernike based integral equations has been recently studied by Sarkisov and Lomba.[45] These authors looked at the behavior of the susceptibilities (compressibility and heat capacities) in the liquid–vapor transition region. Interestingly, it is shown that, in the HNC approximation, the isothermal compressibility tends to diverge as the temperature is lowered. This observation is closely related to the method employed in the present work, in which we approach the critical point by increasing the Debye parameter (playing the role of an inverse temperature). This could explain why the extrapolation procedure employed here performs so

TABLE 3: Critical Parameters of Secondary Minimum Coagulation for the Systems Studied in Ref 10[a]

		ρ^*		κ_c^*	
A (J)	ψ_0 (mV)	ref 10	this work	ref 10	this work
4.83×10^{-20}	20.1	0.063	0.040	36.2	36.2
5.52×10^{-20}	21.6	0.05	0.046	32.5	33.6
1.3×10^{-20}	25	0.05	0.051	121	132

[a] Critical parameters are shown in reduced units ($\kappa^* = \kappa R$ and $\rho^* = \rho R^3$, with R being the colloidal radius).

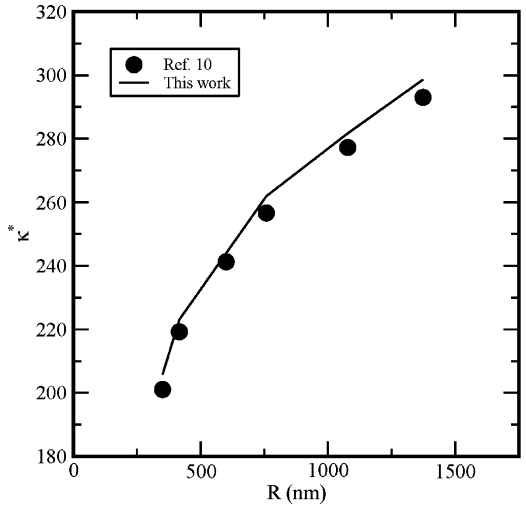

Figure 8. Reduced critical Debye parameter ($\kappa^* = \kappa R$) versus colloidal radius for a colloidal system with $A = 1.3 \times 10^{-20}$ J. The solid line represents the predictions of the method utilized in this work, and the circles stand for the results obtained by solving the full equilibrium conditions.[10]

well when compared with a full computation of the "gas−liquid" coexistence line.

It is interesting to see how the approach to the critical point is reflected in the radial distribution function $g(r)$. The RHNC theory is especially accurate in reproducing the radial distribution functions for pair potentials (including DLVO-like potentials[10]). Bearing this in mind, we present in Figure 4 the $g(r)$'s for successive Debye constants close to the point of critical coagulation in the secondary minimum. As expected, the radial distribution function presents a maximum at the distance at which the secondary minimum or the pair potential is located (see Figure 1). What is more illustrative is that the maximum grows dramatically as we approach the critical point. This feature shows that, in the vicinity of the secondary minimum coagulation, the local concentration of colloids around a particular colloid becomes very high. The mean distance to the central particle also becomes very short with respect to the region away from the coagulation conditions. This particular equilibrium structure of colloids shows how the kinetics of secondary minimum coagulation can become very rapid as we increase the Debye constant. Rate constants of coagulation are computed as a function of the number of encounters that colloidal particles can undergo at specific conditions.[46] The equilibrium $g(r)$ values which are obtained from the RHNC theory can thus serve as a starting point to compute those rate constants.[9]

III. Experimental Section

(a) Materials. In this work, four surfactant-free monodisperse latexes were studied. MP2, Lx1, Lx2, and AS11 latexes were prepared by procedures which have been previously described.[30,47] Lx2 latex was kindly provided by Ikerlat Polymers S.L. (Spain). Some of the main characteristics of the latexes are summarized in Table 1. The latexes were cleaned by serum replacement. Water was purified by reverse osmosis, followed by percolation through charcoal and a mixed bed of ion-exchange resins. The electrolytes used, sodium chloride and calcium chloride, were of analytical grade (Merck) and used as received.

The particle size distribution was determined by transmission electron microscopy (TEM) using an image analysis program (Bolero, AQ systems). All the samples have a polydispersity index (PDI) very near unity, indicating high monodispersity.[48] The weight concentration of the latex was determined gravimetrically. The particle concentration (particles per milliliter) was obtained assuming a density of 1.054 g mL^{-1} for polystyrene and using their TEM diameter.

(b) Measurement of Colloidal Stability and Observation of Secondary Minimum Coagulation ("Repeptization"). The stability ratio (W) in colloid science is usually defined as the ratio of rapid aggregation rate to slow aggregation rate:

$$W = \frac{k_r}{k_s} \tag{13}$$

In the rapid aggregation regime all collisions between particles result in aggregation, whereas in the slow aggregation regime only a fraction of the collisions results in aggregation. Thus, the stability ratio can be considered a delay factor to rapid aggregation or a reciprocal of the aggregation efficiency.

In this work, the stability ratio was obtained experimentally from the rate constant of aggregation of the colloidal particles measured by low-angle light scattering. This technique was developed by Lips and Willis.[49] The scattered light intensity at low angles increases linearly with time, and the aggregation rate can be obtained from its slope if the number of primary particles is known. The scattered light intensity was followed at an angle of 10° during 100 s. The scattering cell shape is rectangular, with a 2-mm path length. Before use the cell was thoroughly cleaned with chromic acid, rinsed with distilled water, and then dried using an infrared lamp. Equal quantities (1 mL) of salt and latex were mixed and introduced in the cell by an automatic mixing device. Dead time is quite short. The latex dispersions used for these aggregation experiments have to be sufficiently dilute to minimize multiple scattering effects, while still having an experimentally convenient coagulation time.

The relation between stability ratios and the electrolyte concentration in the dispersion medium was derived by Reerink and Overbeek.[50] They showed, with several approximations, that a linear relationship between log W and log C_e, where C_e is the electrolyte concentration, could be obtained. The stability ratio decreases with the addition of electrolyte until the electrolyte concentration reaches a critical value just sufficient to bring about rapid aggregation regime. The electrolyte concentration at which W becomes equal to 1 is called the critical coagulation concentration (ccc). Figure 5 shows the dependence of log W with log C_e (for NaCl and $CaCl_2$) for latexes studied in this work. The critical coagulation concentration (ccc) values are summarized in Table 1.

TABLE 4: Critical Salt Concentrations of Secondary Minimum Coagulations for the Colloidal Latexes Studied in Ref 30 and in This Work (See Table 1)

	PS3Ma $D = 99$ nm	S4CS9 $D = 201$ nm	MP2 $D = 360$ nm	Lx1 $D = 414$ nm	Lx2 $D = 530$ nm	AS11 $D = 661$ nm
ψ_0 (mV)	22.5	28.5	35.25	33.4	29.8	31.53
experiment (mM)	no repeptization	150 (NaCl)	10 ($CaCl_2$)	70 (NaCl) 10 ($CaCl_2$)	45 (NaCl)	33 (NaCl)
this work (mM)	750 (1:1) 248 (1:2)	167 (1:1) 55 (1:2)	64 (1:1) 21 (1:2)	59 (1:1) 19 (1:2)	36 (1:1) 12 (1:2)	28 (1:1) 9 (1:2)

As mentioned in the Introduction, coagulation in the secondary minimum should be reversible upon salt dilution since the secondary well can be reduced by decreasing the ionic strength. In this work we detect reversibility by looking at the hydrodynamic diameter of the aggregates as a function of salt concentration. For this purpose we use photon correlation spectroscopy (PCS) to measure mean diffusion coefficients of the particles in the dispersion. The corresponding mean hydrodynamic diameter was calculated from the diffusion coefficient using the Stokes−Einstein equation.[51] If the aggregation occurs in the secondary minimum, the size of the aggregates formed would be reduced by diluting the salt concentration.

The PCS measurements were carried out using a Malvern 4700 system. The reference PCS measuring conditions were a temperature of 25 °C, a scattering angle of 90°, and a wavelength of 488 nm (argon laser). At time zero, equal volumes of latex and salt solution (0.25 mL) were mixed in a test tube. The change in diameter with time was measured using PCS for approximately 3000 s. Then, 2 mL of deionized water was added to the test tube containing the sample and the diameter was measured again.

Table 2 presents repeptization measurements for the latexes. Repeptization exists when the average diameter of aggregates decreases after dilution ("yes"). Figures 6 and 7 show typical experiments to determine repeptization of aggregation upon 1:5 salt dilution. Figure 6 indicates that after dilution the average aggregate diameter does not increase with increasing time. The aggregation process is stopped because of the drastically reduced electrolyte and particle concentration. There is no repeptization after dilution, indicated by the unchanged average aggregate diameter. On the other hand, Figure 7 demonstrates the dilution effect of salt concentration on the mean hydrodynamic diameter of the aggregates when the repeptization phenomenon occurs. When there is repeptization, the average aggregate diameter diminishes after dilution.

IV. Prediction of Secondary Minimum Coagulation Parameters

With the intention of testing the numerical accuracy of the method presented in this work, we have used it to reproduce the results obtained in ref 10. In this paper the authors obtained the full "gas−liquid" coexistence line of various colloidal systems. They used the same modified DLVO potential defined in eq 6. The results showed that the RHNC integral equation, in spite of its numerical limitations in the vicinity of the critical region, improved the prediction of the "gas−liquid" coexistence curve with respect to standard first-order perturbation theory. This was found by comparison with Monte Carlo Gibbs ensemble simulations.

As mentioned, the new method proposed here provides an estimate of the critical coagulation parameters. In Table 3 we present the results for the critical Debye parameter and critical colloidal concentration from the method utilized in ref 10 and the new method described in this work. Three different values of the Hamaker constant and the Stern potential were studied. The new method is particularly accurate in predicting the critical Debye constant, except for the system with the smallest Hamaker constant.

Following ref 10, we have also performed calculations for various colloidal diameters. Results are shown in Figure 8. In this figure it can be seen how the extrapolation method reproduces reasonably well the value of the critical Debye constant obtained from the method of reference. However, small deviations are found. These appear to be more important for big colloids.

Once we have established the performance of the numerical procedure, we have utilized it to make predictions for real colloidal systems which can be modeled with DLVO interaction forces. The experimental data regarding coagulation in the secondary minimum (reversible coagulation) is scarce. However, Molina-Bolívar and co-workers[30] studied thoroughly the transition from irreversible to reversible coagulation (which they called *repeptization*) for four different types of polystyrene latexes. To complement the availability of experimental data, additional results for two more latexes are also presented in this work.

In conformity with previous works,[7,10,15] no reversible coagulation was found for the smallest latex. For larger diameters the suspensions coagulate reversibly at intermediate salt concentrations. At larger concentrations coagulation in the primary minimum dominates and the system aggregates irreversibly. It is interesting to see whether the RHNC−DLVO scheme with the extrapolation procedure devised here is capable of reproducing this behavior. Before doing any calculation regarding the coagulation in the secondary minimum, it is required to fix the value of the Stern potential ψ_0. This can be done by taking into account the fact that coagulation in the primary minimum is normally associated[3,33] with the situation in which the energy barrier of the DLVO potential becomes zero. Hence, using the experimental values of salt concentration for which irreversible concentration was observed (ref 30 and Table 1), we can fix the value of ψ_0 to be used in the RHNC calculations. The values obtained using this procedure can be found in Table 4.

Table 4 also contains the critical salt concentration obtained from the extrapolation procedure described in section II and the values found experimentally. The results are plotted in Figure 9 as a function of the colloidal diameter.

For the smallest latex ($D = 99$ nm) the RHNC predicts reversible coagulation for a salt concentration of 750 mM. This is not observed in the experiment because coagulation in the primary minimum occurs well before reversible coagulation will take place. It must be remembered that the RHNC theory is implemented for the modified DLVO potential defined by eq 6 for which the primary minimum is artificially removed. Hence, the RHNC predictions for secondary minimum coagulation should be always considered in connection with the possibility of primary minimum coagulation if the energy barrier is not large enough. For the latex of diameter 201 nm, the RHNC equation predicts a critical concentration of 167 mM (for 1:1 salt) whereas the experimental value with NaCl is 150 mM.

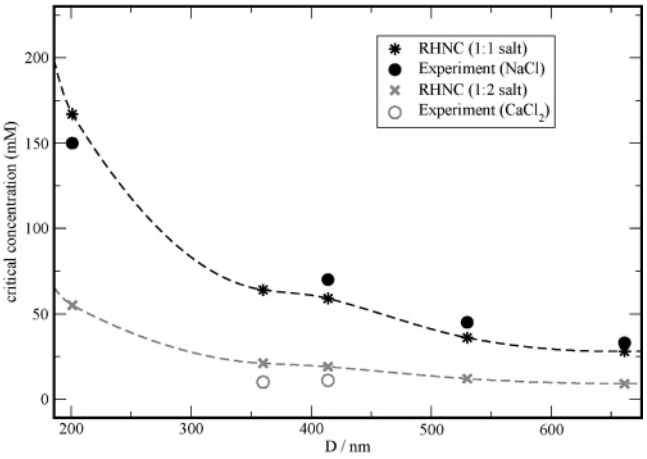

Figure 9. Comparison of theoretical and experimental results for secondary minimum coagulation as a function of colloidal diameter. The dashed lines are spline fittings of the theoretical results.

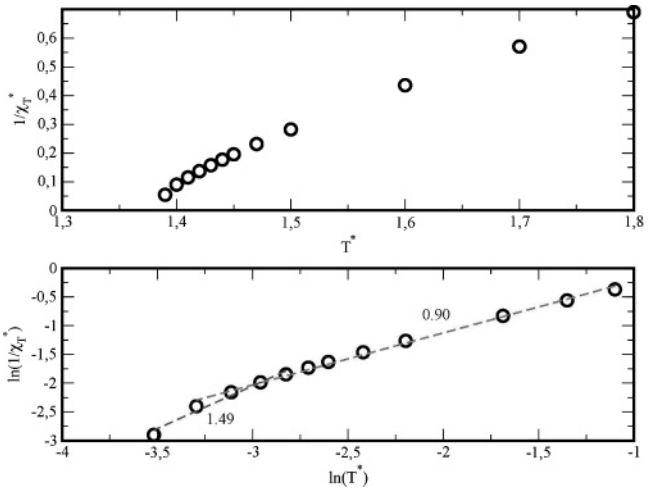

Figure 10. Inverse of the isothermal compressibility in reduced units as a function of the reduced temperature ($T^* = kT/\epsilon$, with ϵ being the energy parameter) as obtained from the solution of the RHNC integral equation for the Lennard-Jones fluid along the critical isochore. Results in linear and double-logarithmic scales are presented. The dashed lines correspond to linear fittings whose slopes (critical exponent) are shown in the graph.

For the rest of the latexes similar good agreement between experiment and theoretical predictions is found.

In summary, knowing the limitations in the computation of the interaction, including the way in which the Stern potential is fixed, this RHNC−DLVO scheme can be considered as fairly accurate to predict stability regions in systems with a secondary minimum.

V. Conclusions

In this work we have devised a theoretical method to estimate the critical parameters of coagulation in the secondary minimum of the DLVO effective potential. For a real situation in which the diameter of the colloid and the Hamaker constant are known, the method can be summarized as follows:

Step 1: Fix the value of the Stern potential by making the energy barrier of the DLVO potential to be zero at the experimental critical salt concentration of irreversible coagulation.

Step 2: The effective DLVO potential is replaced by the modified DLVO potential according to eq 6.

Step 3: The solution of the RHNC integral equation for this modified potential is used to estimate the locus of the critical point. Steps 1−3 in section II are here implemented.

This method is quite rapid (the solution of the integral equation at a given thermodynamic point takes only a few seconds in a standard PC), and it is not affected (apart from numerical errors) by the nonsolution line of the integral equation. It is also quite precise since it reproduces the results obtained previously by the direct application of the "gas−liquid" equilibrium conditions, which allows for the computation of the full coexistence line. In our new method, we just obtain the critical point, but this is sufficient to predict the stability of real colloidal suspensions.

However, it must be pointed out that the method devised here is a *thermodynamic* technique and its predictions rely on the assumption that the system is in *equilibrium*. We have seen that this assumption is reasonable if the energy barrier of the DLVO potential is high enough with respect to the average thermal energy of the colloidal particles. A more rigorous description based on kinetic considerations such as that utilized in ref 9 would be needed in this context. Nevertheless, the thermodynamic description would be very useful as a means to obtain the upper limit of reversible coagulation in conditions of *pseudoequilibrium.* The radial distribution functions which can be obtained from the solution of the RHNC equation can also be utilized to develop more realistic rate constants of coagulation. It can also be very useful in the description of non-DLVO systems[52] in which there is no primary minimum and the system can be regarded as a true equilibrium system.

Acknowledgment. The authors wish to thank Prof. R. Hidalgo-Álvarez, Group of Fluid Physics and Biocolloids, for providing the opportunity to perform the light scattering experiments at the University of Granada and Victor Morales, University of Cadiz, for discussions and technical reports. J.A.A. and M.C. thank the Ministerio de Educación y Ciencia of Spain for financial support under Grant ENE2004-01657/ALT and for a Ph.D. studentship.

Appendix: Estimation of the Critical Point for the Lennard-Jones System

The Lennard-Jones potential[19] provides an adequate benchmark to check the precision of the extrapolation procedure proposed here. An accurate estimation of the critical parameters of the Lennard-Jones fluid has been obtained by Potoff and Panagiotopoulos.[53] These authors report 1.3120 ± 0.0007 and 0.316 ± 0.001 for the critical temperature ($T^* = kT/\epsilon$) and the critical density ($\rho^* = \rho\sigma^3$), respectively.

We have used the extrapolation procedure described in section II.c to estimate the critical parameters of the Lennard-Jones fluid. The following values are obtained for the critical density and the critical temperature: $\rho^* \approx 0.30$ and $T^* \approx 1.36$. As it is well-known in the context of HNC-like theories,[20,22] the integral equation slightly *overestimates* the critical temperature.

In order to illustrate the descent along the critical isochore, we have plotted in Figure 10 RHNC results for the inverse of the isothermal compressibility as a function of temperature, in both linear and double-logarithmic scales. It is observed that the RHNC results approach the critical limit with a classical critical exponent of $\gamma \approx 1$. Nevertheless, very close to the nonsolution boundary, the RHNC results bend toward smaller values of $1/\chi_T$, so that the critical exponent approaches the Ising value of $\gamma = 1.33$. A similar effect has been reported by Abramo and Caccamo.[43] In any case, as can be inferred from the graph, the error produced when using either classical or Ising critical

exponents is very small as far as the estimation of the critical temperature is concerned. Furthermore, no significant variation of the results is observed when a finer grid is utilized (say, 8192 or 16 384 points with smaller grid sizes).

References and Notes

(1) Evans, D. F.; Wennerström, H. *The Colloidal Domain, where Physics, Chemistry, Biology and Technlogy meet*; Wiley-VCH: New York, 1999.
(2) Derjaguin, B. V.; Landau, L. D. *Acta Physicoquim. URSS* **1941**, *14*, 633.
(3) Verwey, E. J. W.; Overbeek, J. Th. G. *Theory of the Stability of Lyophobic Colloids*; Elsevier: Amsterdam, 1948.
(4) Grimson, M. J. *J. Chem. Soc., Faraday Trans. 2* **1983**, *79*, 817.
(5) Victor, J. M.; Hansen, J. P. *J. Chem. Soc., Faraday Trans. 2* **1985**, *81*, 43.
(6) Kaldasch, J.; Laven, J.; Stein, H. N. *Langmuir* **1996**, *12*, 6197.
(7) Lai, S. K.; Peng, W. P.; Wang, G. F. *Phys. Rev. E* **2001**, *63*, 41511.
(8) Lai, S. K.; Wu, K. L. *Phys. Rev. E* **2002**, *66*, 041403-1.
(9) Wu, K. L.; Lai, S. K. *Langmuir* **2005**, *21*, 3238.
(10) Morales, V.; Anta, J. A.; Lago, S. *Langmuir* **2003**, *19*, 475.
(11) Frens, G.; Overbeek, J. Th. G. *J. Colloid Interface Sci.* **1972**, *38*, 376.
(12) Jeffrey, G. C.; Ottewill, R. H. *Colloid Polym. Sci.* **1988**, *266*, 173.
(13) Litton, G. M.; Olson, T. M. *Colloids Surf., A* **1996**, *107*, 273.
(14) Minimi, H.; Inoue, T.; Shimozaya, R. *Langmuir* **1996**, *12*, 3574.
(15) Kotera, A.; Furosawa, K.; Kubo, K. *Kolloid Z. Z. Polym.* **1970**, *240*, 837.
(16) Urbina-Villalba, G.; García-Sucre, M. *Langmuir* **2005**, *21*, 6675.
(17) Liu, J.; Zhang, L.; Xu, Z.; Masliyah, J. *Langmuir* **2006**, *22*, 1485.
(18) Hahn, M. W.; Abadzic, D. A.; Melia, C. R. *Environ. Sci. Technol.* **2004**, *38*, 5915.
(19) Hansen, J.-P.; McDonald, I. R. *Theory of Simple Liquids*; Academic Press: London, 1986.
(20) Caccamo, C. *Phys. Rep.* **1996**, *274*, 1−105.
(21) Lado, F. *Phys. Rev. A* **1973**, *8*, 245.
(22) Lomba, E. *Mol. Phys.* **1989**, *68*, 87.
(23) Lomba, E.; Almarza, N. G. *J. Chem. Phys.* **1994**, *100*, 8367.
(24) See, e.g.: Hasegawa, M.; Hoshino, K.; Watabe, M.; Young, W. H. *J. Non-Cryst. Solids* **1990**, *117*−*118*, 300. González, L. E.; Meyer, A.; Iñiguez, M. P.; González, D. J.; Silbert, M. *Phys. Rev. E* **1993**, *47*, 4120. Anta, J. A.; Louis, A. A. *Phys. Rev. B* **2000**, *61*, 11400.
(25) See, e.g.: Fries, P. H.; Patey, G. N. *J. Chem. Phys.* **1985**, *88*, 429.
(26) See, e.g.: Caccamo, C.; Giunta, G.; Malescio, G. *Mol. Phys.* **1995**, *84*, 125. Anta, J. A.; Lomba, E.; Alvarez, M.; Lombardero, M.; Martín, C. *J. Phys. Chem. B* **1995**, *101*, 1451.
(27) Anta, J. A.; Lago, S. *J. Chem. Phys.* **2002**, *116*, 10514.
(28) Anta, J. A. *J. Phys: Condens. Matter* **2005**, *17*, 7935.
(29) Belloni, L. *J. Phys.: Condens. Matter* **2000**, *12*, R549.
(30) Molina-Bolívar, J. A.; Galisteo-González, F.; Hidalgo-Álvarez, R. *J. Colloid Interface Sci.* **1997**, *195*, 289.
(31) Louis, A. A. *J. Phys.: Condens. Matter* **2002**, *14*, 9187.
(32) van Roij, R.; Dijkstra, M.; Hansen, J.-P. *Phys. Rev. E* **1999**, *59*, 2010.
(33) Anta, J. A.; Lago, S. *J. Chem. Phys.* **2002**, *116*, 10514.
(34) See, e.g.: Xu, H.; Hansen, J.-P. *Phys. Rev. E* **1998**, *57*, 211. Anta, J. A.; Louis, A. A. *Phys. Rev. B* **2000**, *61*, 11400.
(35) Rosenfeld, Y.; Ashcroft, N. W. *Phys. Rev. A* **1979**, *20*, 1208.
(36) Lado, F. *Phys. Rev. A* **1973**, *8*, 245.
(37) Lado, F.; Foiles, S. M.; Ashcroft, N. W. *Phys. Rev. A* **1983**, *28*, 2374.
(38) Verlet, L.; Weis, J. J. *Phys. Rev. A* **1972**, *5*, 939.
(39) Labík, S.; Malyjevský, A. *Mol. Phys.* **1989**, *67*, 431.
(40) Ng, K. *J. Chem. Phys.* **1974**, *61*, 2680.
(41) Broyles, A. A. *J. Chem. Phys.* **1960**, *33*, 2680.
(42) Binney, J. J.; et al. *The Theory of Critical Phenomena*; Clarendon Press: Oxford, 1999.
(43) Abramo, M. C.; Caccamo, C. *Phys. Lett.* **1992**, *A166*, 70.
(44) Belloni, L. *Phys. Rev. Lett.* **1986**, *57*, 2026. Belloni, L. *J. Chem. Phys.* **1993**, *98*, 8080.
(45) Sarkisov, G.; Lomba, E. *J. Chem. Phys.* **2005**, *122*, 214504.
(46) Russel, W. B.; Saville, D. A.; Schowalter, W. R. *Colloidal Dispersions*; Cambridge University Press: New York, 1989.
(47) Romero-Cano, M. S.; Martín-Rodríguez, A.; Chauveteau, G.; de las Nieves, F. J. *J. Colloid Interface Sci.* **1998**, *198*, 266.
(48) Tsaur, S. L.; Ficht, R. M. *J. Colloid Interface Sci.* **1987**, *115*, 450.
(49) Lips, A.; Willis, E. J. *J. Chem. Soc., Faraday Trans. 1* **1971**, *67*, 2979.
(50) Reerink, H.; Overbeek, J. Th. *Discuss. Faraday Soc.* **1954**, *18*, 74.
(51) Pecora, R. In *Measurement of Suspended Particles by Quasi-elastic Light Scattering*; Dahneke, B. E., Ed.; Wiley: New York, 1983; p 3.
(52) See, for instance: Edwards, J.; Everett, D. H.; O'Sullivan, T.; Pangalou, I.; Vincent, B. *J. Chem. Soc., Faraday Trans. 1* **1984**, *80*, 2599.
(53) Potoff, J. J.; Panagiotopoulos, A. Z. *J. Chem. Phys.* **1998**, *109*, 10914.